CHEESA: Chemical Engineering Research Articles
ISSN 2614-8757 (Print), ISSN 2615-2347 (Online)
Homepage: https://e-journal.unipma.ac.id/index.php/cheesa

Research Article

OPEN ACCESS

CHEESA, 9(1), pp 15-25, 2026

Thermoplastic Elastomers of Polystyrene-Based Reinforced with Natural Rubber and Carbon Filler from Oil Palm Empty Fruit Bunches

Indah Agus Setiorini[1*)], Achmad Faisal Faputri[1)], Rahma Nuryanti[1)], Amiliza Miarti[1)], Muhammad Rasyad Hilmi[2)], Hasrinah Hasbullah[3)]

[1)]Politeknik Akamigas Palembang, Department of Chemical Engineering, Jl. Kebon. Jahe, Komperta, Kec. Plaju, Palembang City, Sumatera Selatan, 30268, Indonesia

[2)]Head of HRD at a Rubber Processing Company, JI. Ki Kemas Rindo, Kec. Kertapati, Palembang City, Sumatera Selatan, 30258, Indonesia

[3)]Universiti Teknologi Malaysia, Faculty of Chemical and Energy Engineering, 81310 UTM Johor Bahru, Johor, Malaysia

*corresponding author: indah@pap.ac.id

Article History

Submitted: 24th October 2025; Revised: 26th April 2026; Accepted: 07th May 2026;

Available online: 03rd June 2026; Published Regularly: June 2026

doi: 10.25273/cheesa.v9i1.23348.15-25

Abstract

Polystyrene (PS) has limited resistance to extreme temperatures, often becoming soft, brittle, and losing its elasticity. To address these limitations, the material was modified by adding Natural Rubber (NR) and oil palm empty fruit bunch (OPEFB) carbon filler. Therefore, this research aimed to modify the surface of PS by adding NR and OPEFB carbon filler, followed by analysis of the resulting morphology, thermal stability, and enthalpy change (ΔH) of the composites. The polystyrene grafting with maleic anhydride (PS-g-MA) was carried out at 75 °C for 10 minutes. The composition variations of PS-g-MA/NR/OPEFB carbon filler were (30:65:5) wt%, (30:60:10) wt%, (30:55:15) wt%, (30:50:20) wt%, and (30:45:25) wt%. The highest thermal stability ($T_{5\%}$) was achieved with 10% filler at 363°C. However, morphological analysis showed that increasing the filler content to 20% provides an optimal point in balancing interfacial interaction (maximum adhesion) and phase dispersion, with a ΔH value of -27.86 J/g.

Keywords: filler; natural rubber; oil palm empty fruit bunches; polystyrene; thermoplastic elastomer

1. Introduction

Polymeric materials are widely recognized in the packaging industry for their high stability, low density, and flexibility. Polystyrene (PS) is a nonpolar synthetic polymer widely used in the packaging industry due to its low cost, transparency, and flexibility [1]-[3]. However, PS still has disadvantages, including low flexibility, brittleness, and non-biodegradability [4]. To improve the thermal stability and mechanical properties of PS, researchers have modified PS copolymers with the polar comonomer Maleic Anhydride (MA), elastomeric modification using Natural Rubber (NR), and carbon fillers from Oil Palm Empty Fruit Bunches (OPEFB).

Natural Rubber (NR) is a natural resource abundant in Indonesia, and its uses replace relatively expensive imported synthetic rubber. The use of OPEFB carbon filler represents an effort to support a green economy through the valorization of OPEFB waste. The elastomeric modification of NR combined with OPEFB carbon filler is expected to improve the composite morphology and thermal stability of the material, as well as facilitate the degradation of PS polymers, thereby addressing challenges in the packaging industry. Efforts to manufacture PS and NR-based thermoplastic elastomers are expected to approach the standards required by the polymer industry.

Previous research reported the use of inorganic fillers, such as carbon nanotubes, which posed challenges to achieving effective dispersion [5]. In response, environmentally friendly and biodegradable organic fillers, such as hemp shives and OPEFB-derived carbon, have been explored as viable alternatives [6]-[8]. Blending PS with other

This is an open access article under the CC BY license (http://creativecommons.org/licenses/by/4.0/)

polymers or fillers, including Halloysite nanotubes (HNT) and surface-modified biochar in polypropylene (PP)/acrylonitrile butadiene styrene (ABS) systems, has been shown to mitigate the inherent limitations of PS [9],[10]. Elastomeric modification using polyolefin elastomers (POE), such as ethylene–butene rubber (EBR) and ethylene–octene copolymer (EOC), has also been investigated, although the resulting PS/POE blends often exhibit reduced tensile strength and Young's modulus [11]-[13]. Additional investigations examined the effect of ZnO nanopowder filler on the dielectric properties of PS matrices [14], applying 2D MXene–organic hybrid nanomaterials (O-Ti3C2) to PS as a nanofiller [15], and modifying nanocomposites into polypropylene/multiwalled carbon nanotubes-graft-polystyrene (PP/MWCNTs-g-PS) nanoalloys [16].

A chemical modification of PS was carried out by grafting with maleic anhydride (MA) and inducing controlled degradation using benzoyl peroxide (BPO) prior to composite preparation. This pre-treatment was intended to enhance compatibility with natural rubber (NR) and OPEFB carbon filler during subsequent blending. The treatment substantially improved the dispersion of NR and OPEFB carbon fillers, enhanced interfacial compatibility within the PS matrix, and improved the mechanical properties of the composites [17]. This comprehensive exploration is essential for guiding researchers in tailoring surface modification strategies to achieve optimal compatibility among PS, NR, and OPEFB carbon fillers, while ensuring uniform and stable dispersion within the polymer matrix.

The resulting composite of PS, NR, and OPEFB carbon filler is expected to have applications across various thermoplastic elastomer-based industries, including automotive, household appliances, medical devices, packaging, footwear, children's toys, and cables. Therefore, this research aimed to identify new methods to mitigate the weaknesses of thermoplastic elastomers derived from blends of PS, NR, and OPEFB carbon filler, as well as to provide relevant, scientifically based solutions for developing high-performance, sustainable thermoplastic elastomers from renewable sources. The novelty of this research is the functional use of OPEFB-based carbon filler not only as a mechanical reinforcement agent but also as a morphological stabilizer, thereby enhancing thermal stability.

2. Research Methods

2.1. Tools and Materials

In this research, the materials used consisted of PS monomer from a chemical distributor in West Jakarta, NR SIR 10 from PT. X, a rubber industry in South Sumatra, OPEFB carbon filler from PT. Y, one of the palm oil industries in Musi Banyuasin Regency, Maleic Anhydride 99% Merck, Benzoyl Peroxide (BPO) 75%, and Toluene Analyst 95-98% Merck from PT. SMART LAB Indonesia is a regional chemical distributor in Palembang City.

A composite morphology test was performed using a JEOL Scanning Electron Microscope (SEM) Type JED-2300 Analysis Station. A melting point test was conducted using a Shimadzu Differential Scanning Calorimetry (DSC) Type DSC-60 Plus series C30935200137SA. Moreover, a thermal stability test was performed using a Shimadzu Thermogravimetric Analysis-Differential Thermal Analysis (TGA/DTA) Type DTG-60, series C30566100979TK.

2.2. Thermoplastic Elastomers (TPE) of Polystyrene Preparation

The TPE composite modification was carried out in four main stages with five variations, and PS/NR/OPEFB composition ratios are shown in Table 1.

2.2.1. PS Degradation with BPO Initiator

The PS was first prepared and weighed as needed. Subsequently, the PS was mixed with BPO as an initiator at a (90:10) wt% PS: BPO ratio in a glass beaker and heated on a hotplate at 75°C for 10 minutes with stirring until homogeneous. After the degradation process was complete, the mixture was cooled to 32°C before being used in the next step.

2.2.2. Grafting PS with Maleic Anhydride (MA) / (PS-g-MA)

The degraded PS was subsequently prepared for grafting. PS, MA, and BPO were measured in a weight ratio of 92:6:2, respectively. Grafting was performed in a glass beaker at 75 °C for 10 minutes under continuous stirring to ensure a homogeneous mixture. After the process was complete, the mixture was cooled to room temperature before being used in the next step. Grafting polystyrene with maleic anhydride (PS-g-MA) was carried out via reactive processing using BPO as the initiator.

Table 1. Variations of oil palm empty fruit bunches (OPEFB) and natural rubber with 30% polystyrene grafting maleic anhydride (PS-g-MA)

Composition	Mixture (wt%)				
	TPE_1	**TPE_2**	**TPE_3**	**TPE_4**	**TPE_5**
PS-g-MA	30	30	30	30	30
Natural Rubber	65	60	55	50	45
OPEFB Carbon Filler	5	10	15	20	25

2.2.3. Mixing OPEFB Carbon Filler with NR

The 200-mesh OPEFB carbon filler and NR were weighed according to the specified formulation, consisting of 5 g OPEFB carbon filler and 65 g NR (TPE_1). The components were then blended in a beaker using an internal mixer at 32 °C and a stirring speed of 60 rpm for 20 minutes. However, the NR was first dissolved in toluene at a (1:3) wt% ratio, which acts as a molecular expander for the NR, thereby optimizing the interaction between the OPEFB carbon filler and the NR matrix. After the mixing process was complete, the resulting mixture was prepared for the final mixing stage with PS-g-MA.

2.2.4. Mixing PS-g-MA, NR, and OPEFB Carbon Filler

The PS-g-MA, NR, and OPEFB carbon filler composites were mixed in a glass beaker using an internal mixer at 32 °C and a stirring speed of 60 rpm for 20 minutes, with varying ratios. They were then formed into sheets using a molding and drying process, after which morphological and thermal tests were conducted.

2.3. Composite Analysis

A composite morphology test was performed using SEM at 3000x magnification and a 5µm scale. A melting point test was performed using DSC at a heating rate of 10 °C/min and a nitrogen flow rate of 10 ml/min at the LPPT Testing Laboratory, Gadjah Mada University. A thermal stability test was performed using TGA/DTA at a heating rate of 10°C/min and a nitrogen flow rate of 50 ml/min at the Integrated Laboratory of the Sumatra Institute of Technology.

3. Results and Discussion

3.1. TPE Composite Morphology Analysis

Figure 1 shows the effect of compatibilizer (PS-g-MA) and filler addition. Increasing the filler content reduces the formation of voids at the interface, and at higher loadings, these voids may be eliminated entirely. In addition, the agglomeration of PS and NR decreases, while interfacial adhesion between the two phases is improved. The incorporation of OPEFB carbon filler enhances phase distribution and promotes greater composite homogeneity. The presence of small, uniformly distributed domains further indicates good interfacial compatibility, which can be attributed to the effect of the compatibilizer [18],[19].

Voids were formed in TPE_1 due to imperfect mixing and phase separation between PS and NR. The resulting voids typically reduce mechanical strength and can serve as crack initiation points. The thin, stretched fiber-like structure indicates the possibility of a continuous NR elastomeric phase. The denser areas likely correspond to domains of the harder, more brittle PS phase [20]-[24]. These morphological differences indicate the presence of phase-separated microphases, which are characteristic of chemically incompatible polymer blends. In each composite, the fine, densely distributed particles embedded within the matrix are likely OPEFB carbon filler. The uniform dispersion of the filler within the matrix suggests effective integration and strong interfacial adhesion.

Based on the voids formed and the total ΔH required during degradation (Table 4), Figures 2 and 3 represent the best composite mapping of TPE_4. The minimal voids directly contribute to the thermal stability, as shown by the increase in the total ΔH value to -27.86 J/g compared to TPE_1, TPE_2, TPE_3, and TPE_5. Table 2 shows that the C element in the PS-g-MA/NR/OPEFB carbon filler composite of TPE_4 is very dominant and evenly distributed, as expected. This is shown by the EDS spectrum showing a characteristic C energy peak at 0.277 keV (Figure 3) with the highest intensity because PS, NR, and the carbon filler are all carbon-based, indicated by the blue color (Figure 2), with a carbon content of 73.82% by weight and 80.03% by atoms. The figure indicates the EDS spectrum, showing peaks for Mg at 1,253 keV, K at 3,312 keV, and Ca at 3,690 keV, indicating the presence of mineral residues from the carbonization process or inorganic ash from biomass, which are natural mineral components of OPEFB [25]. The presence of these elements is indicated by

the orange, yellow, and golden yellow colors (Figure 2).

The N energy at 0.392 keV (Figure 3) originates from filler functional groups [26], representing minor contamination from organic compound residues and influencing interphase interactions in the composite material, indicated by the light blue color (Figure 2). The filler distribution is not entirely homogeneous, as indicated by the localized accumulation of inorganic elements in certain regions. However, no evidence of heavy metal contamination or foreign impurities was observed, suggesting that the composite is chemically clean. This non-uniform distribution may result in localized variations in mechanical properties, including stiffness and tensile strength.

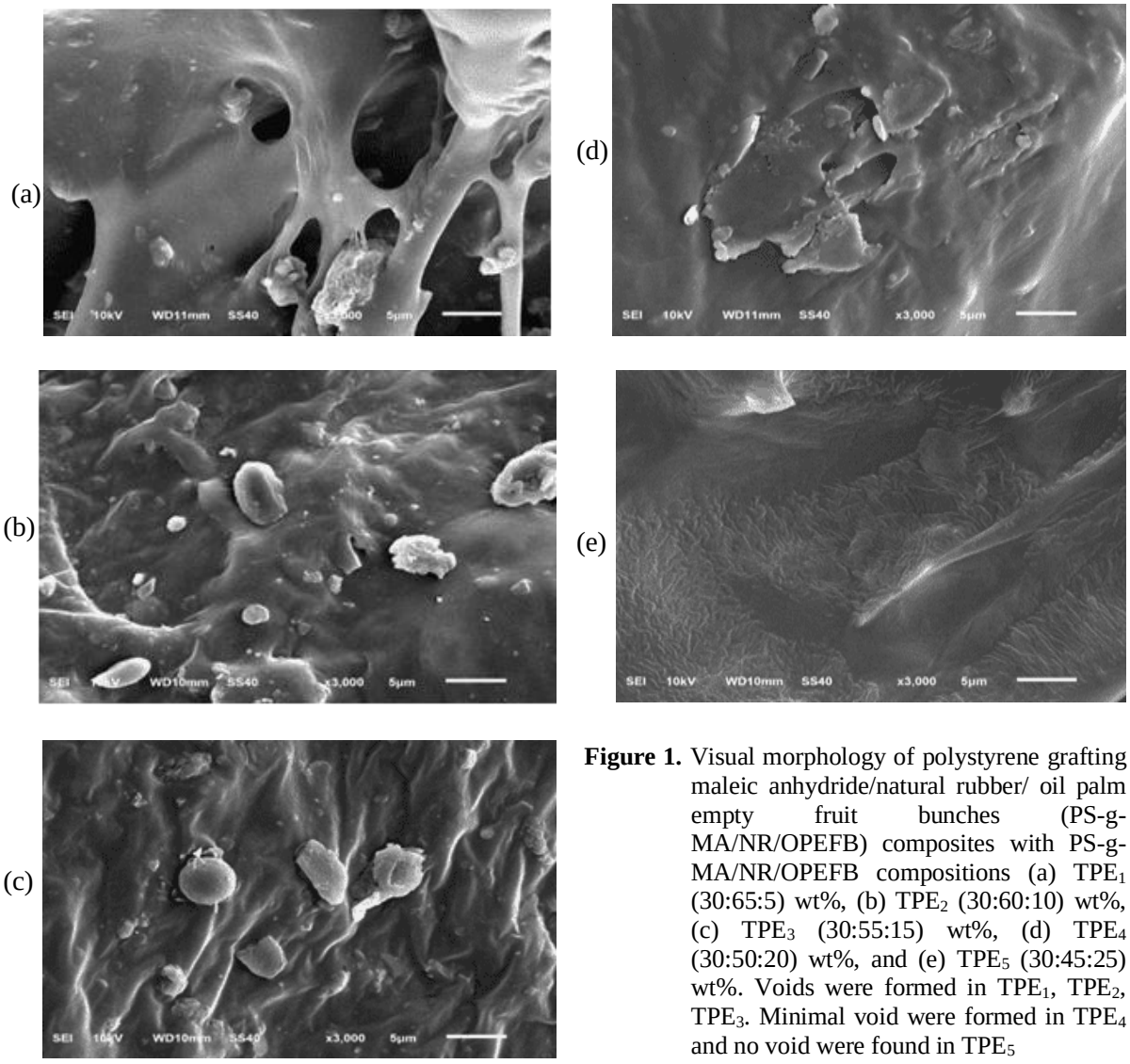

Figure 1. Visual morphology of polystyrene grafting maleic anhydride/natural rubber/ oil palm empty fruit bunches (PS-g-MA/NR/OPEFB) composites with PS-g-MA/NR/OPEFB compositions (a) TPE_1 (30:65:5) wt%, (b) TPE_2 (30:60:10) wt%, (c) TPE_3 (30:55:15) wt%, (d) TPE_4 (30:50:20) wt%, and (e) TPE_5 (30:45:25) wt%. Voids were formed in TPE_1, TPE_2, TPE_3. Minimal void were formed in TPE_4 and no void were found in TPE_5

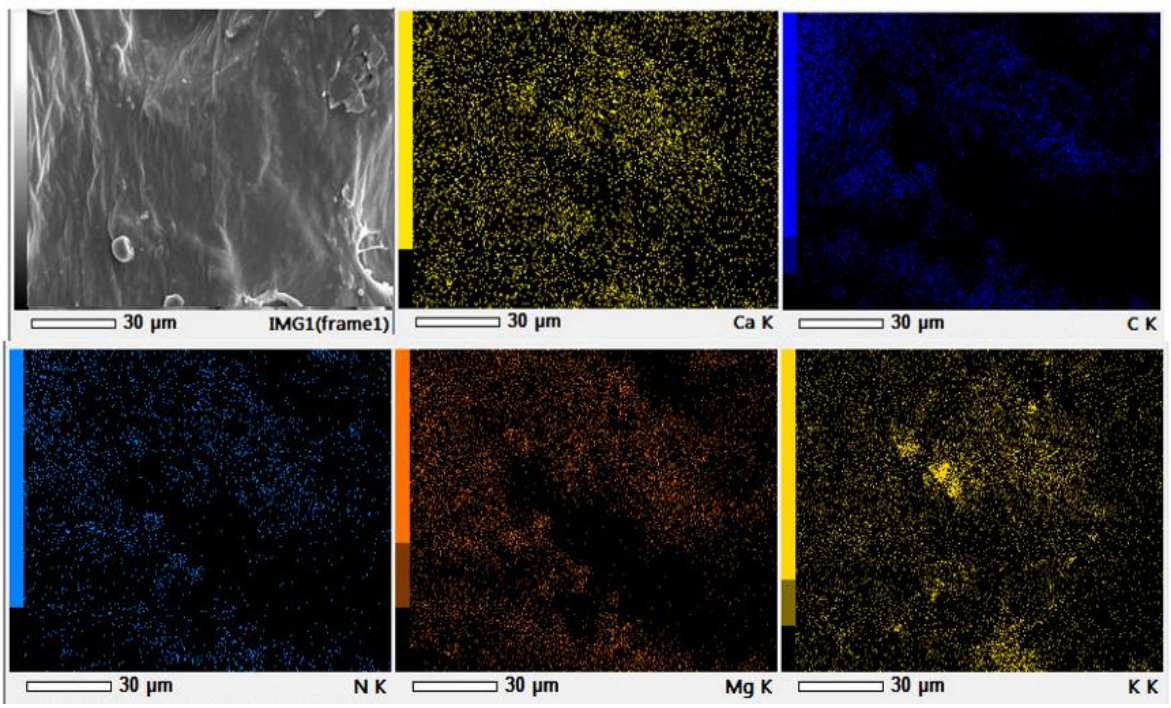

Figure 2. Mapping of polystyrene grafting maleic anhydride/natural rubber/ oil palm empty fruit bunches (PS-g-MA/NR/OPEFB) composites in TPE_4 (30:50:20) wt%

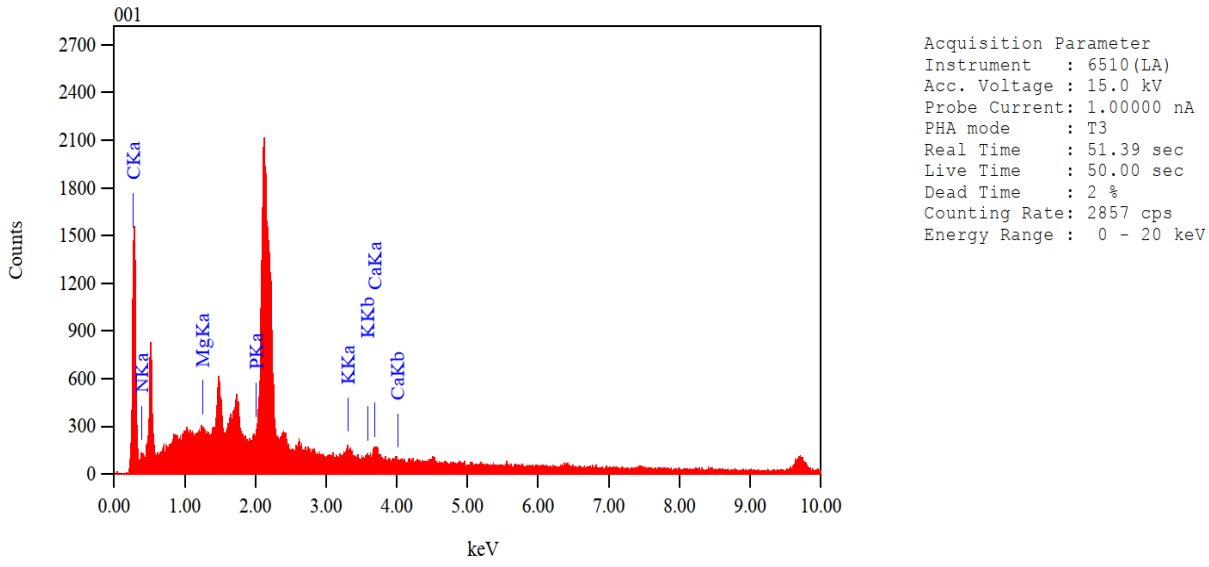

Figure 3. Elemental composition mapping of polystyrene grafting maleic anhydride/natural rubber/ oil palm empty fruit bunches (PS-g-MA/NR/OPEFB) composites in TPE_4 (30:50:20) wt%

Table 2. Elemental mapping data of polystyrene grafting maleic anhydride/natural rubber/ oil palm empty fruit bunches (PS-g-MA/NR/OPEFB) composites in TPE_4 (30:50:20) wt%

Element	Energy (keV)	% Weight	% Atoms	Interpretation[27],[28]
C	0.277	73.82	81.03	Polymer matrix & carbon filler
N	0.392	16.27	15.31	Functional groups of polymer matrix or organic compound residue
Mg	1.253	1.75	0.95	Ash/filler impurity/biomass source
K	3.312	3.40	1.15	Ash/filler impurity/biomass source
Ca	3.690	4.76	1.57	Ash/filler impurity/biomass source

3.2. Thermogravimetric Analysis – Differential Thermal Analysis (TGA/DTA)

OPEFB carbon filler contains cellulose, hemicellulose, and lignin, which undergo gradual degradation from 200–400°C depending on its composition [29],[30]. PS is a rigid and brittle aromatic thermoplastic with a degradation temperature of around 350–450°C. NR is a flexible elastomer that degrades at 250–400°C [31],[32]. The addition of a carbon filler can improve phase distribution and interphase compatibility, resulting in more homogeneous interfacial adhesion [33]. However, the addition of filler can result in solid residue in the form of inorganic biomass ash derived from the natural mineral components of the OPEFB, leading to multi-stage degradation.

The thermal stability and remaining solid residue values of the PS-g-MA/NR/OPEFB carbon filler composite, along with the initial decomposition temperature (T_{onset}), and the peak temperature at the maximum decomposition rate (T_{Peak} or T_{max}) obtained from the TGA/DTA curves, are presented in Table 3. A residual mass of less than 10% in the TGA/DTA analysis indicates that the PS-g-MA/NR/OPEFB carbon filler composite contains a low level of inorganic or mineral content. This is consistent with its predominantly organic composition, which undergoes substantial thermal decomposition with increasing temperature, as reflected by the progressive mass loss.

The absence of significant residue at the end of heating (>500°C) indicates near-complete decomposition of the grafted polymer matrix (PS-g-MA) and filler. Because it is difficult to determine the exact onset of degradation (T_{onset}), the temperature at 5% mass loss ($T_{5\%}$) is used as a reference for assessing the material's thermal stability. $T_{5\%}$ is the temperature at which the TPE mass decreases by 5% of its initial mass.

The PS-g-MA/NR/OPEFB carbon filler composite exhibits good thermal stability ($T_{5\%}$) up to approximately 300°C–360°C. The higher the thermal stability temperature, the more heat-resistant the composite [34]. The main degradation (T_{Peak}) occurs at approximately 450–470°C, corresponding to the decomposition of the PS and NR matrices under the influence of the filler. The addition of OPEFB filler lowers the initial degradation temperature (T_{onset}) but does not significantly alter the degradation mechanism. Significant degradation occurs at high filler levels of 20% and 25%.

The best thermally stable TPE are those with moderate filler proportions of 5% and 10%, where the interaction between the matrix and filler is most balanced. The PS-g-MA/NR/OPEFB carbon filler composite begins to degrade at 350°C, with significant degradation around 360°C and the highest degradation rate at 460°C, the maximum point of the decomposition reaction.

At these moderate compositions (5% and 10%), fillers and compatibilizers can improve initial heat resistance by acting as thermal barriers at the composite surface. With higher OPEFB filler content, the T_{onset} and T_{Peak} shift toward lower values, indicating a reduction in thermal stability. This behavior is attributed to the presence of more thermally labile components in the filler, such as cellulose, hemicellulose, and lignin, which decompose more readily at elevated temperatures [7],[8],[35],[36].

3.3 Differential Scanning Calorimetry (DSC) Analysis

DSC analysis is performed to determine the heat changes accompanying thermal transitions in composites, such as T_{onset} or the glass transition (T_g), as indicated by steps in the heat flow curve, melting (T_m), or exothermic/endothermic reactions (ΔH). For the PS-g-MA/NR/OPEFB carbon filler composite system, DSC results demonstrate how filler interactions affect polymer chain stability and mobility.

Table 3. T_{onset}, $T_{5\%}$, T_{peak}, and Residue of the polystyrene grafting maleic anhydride/natural rubber/ oil palm empty fruit bunches (PS-g-MA/NR/OPEFB) composites

Composite Code	Main Composition (wt%)	T_{onset} (°C)	$T_{5\%}$ (°C)	T_{Peak} (°C)	Residue (%)
TPE_1	30 PS + 65 NR + 5 OPEFB carbon filler	358	360	468	2.3
TPE_2	30 PS + 60 NR + 10 OPEFB carbon filler	351	363	471	2.3
TPE_3	30 PS + 55 NR + 15 OPEFB carbon filler	335	341	466	2.4
TPE_4	30 PS + 50 NR + 20 OPEFB carbon filler	315	331	460	2.5
TPE_5	30 PS + 45 NR + 25 OPEFB carbon filler	305	329	439	2.6

Figure 4 shows several peaks in the 140–180 °C range, including downward endothermic peaks at heating rates of -2.8 to -3.8 mW, indicating heat-absorption activity [37]. The different thermal responses among composites indicate system heterogeneity, meaning the material contains more than one thermally active phase. This indicates partial mixing within the PS-g-MA/NR/OPEFB carbon filler composites, in which the components are not completely homogenized at the particle level but exist as distinct phases. However, these phases remain bonded and interact with each other, contributing to mutual reinforcement within the composite structure [38]-[40]**.** The system exhibits a broad, non-uniform T_g, indicating amorphous structural heterogeneity, with a relatively smooth baseline shift in the 70–170 °C range (varying among composites) [41].

The addition of an MA compatibilizer and an OPEFB carbon filler resulted in numerous peaks appearing, indicating that they alter the internal structure and interphase interactions [42]. Table 4 shows that the ΔH values increase from TPE_1 to TPE_4, indicating that the transition process requires more energy. This suggests that thermal stability is enhanced by the presence of the carbon filler, which restricts the molecular chain mobility within the PS-g-MA/NR/OPEFB carbon filler composites. The improvement in thermal stability further indicates the formation of an effective filler–polymer network, which significantly limits the movement of the PS-g-MA/NR chains. However, in TPE_5, the ΔH value decreases, indicating excessive filler agglomeration, thereby reducing filler-polymer interactions. This phenomenon indicates the presence of an optimum filler content, where the balance between filler dispersion is appropriate for producing a mixture with optimal performance.

A peak temperature shift (T_m) of more than one and a wider T_{Onset}–T_{Endset} range indicates multiphase formation (Table 4). TPE_1 to TPE_4 show optimal multiphase formation, with the interphases still interacting, as evidenced by the high energy required to break the composite interface. The OPEFB carbon filler increases polymer chain rigidity and restricts thermal mobility, thereby shifting the transition to higher temperatures. In TPE_5, the multiphase structure becomes more fragmented, with each phase undergoing its own transition. As a result, the transition energy is distributed over a broader range, as reflected by the reduction in total ΔH to −23.86 J/g. This decrease is attributed to filler agglomeration, which intensifies multiphase behavior within the composite. This is due to the formation of an effective thermally conductive network within the matrix, which accelerates the thermal degradation of the polymer phase [43],[44]. For TPE_2, less homogeneous mixing occurs, leading to weak filler-polymer interactions and poor dispersion, resulting in decreases in T_g and T_m of 72.1°C and 76.8°C (more flexible chains) [41].

DSC analysis of the PS-g-MA/NR/OPEFB carbon filler composite shows that the grafting process and the addition of OPEFB carbon filler increase the peak temperature (T_m) and enthalpy (ΔH), indicating greater thermal stability and enhanced filler-polymer matrix interactions. At higher compositions, several transition peaks appear, indicating a multiphase system, but it is more heat-stable than the composite with the lowest filler content. Detailed T_g, T_m, T_{Endset}, and ΔH values are shown in Table 4.

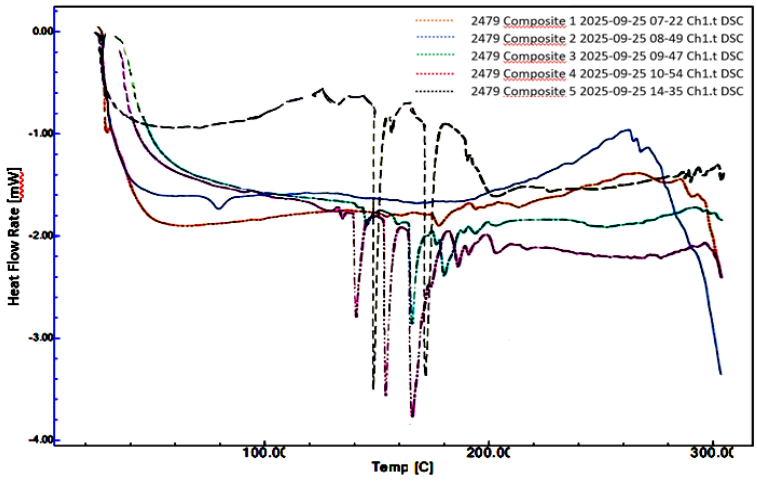

Figure 4. Differential Scanning Calorimetry (DSC) Curves of the polystyrene grafting maleic anhydride/natural rubber/ oil palm empty fruit bunches (PS-g-MA/NR/OPEFB) composites

Table 4. T_g and T_m Values of the polystyrene grafting maleic anhydride/natural rubber/ oil palm empty fruit bunches (PS-g-MA/NR/OPEFB) composites

Composite Code	Main Composition (wt%)	T_m (°C)	T_g (°C)	T_{Endset} (°C)	ΔH (J/g)	ΔH_{total}(J/g)
TPE_1	30 PS + 65 NR + 5 OPEFB carbon filler	175.5	172.5	180.3	−1.11	−1.11
TPE_2	30 PS + 60 NR + 10 OPEFB carbon filler	76.8	72.1	81.6	−1.41	−1.41
TPE_3	30 PS + 55 NR + 15 OPEFB carbon filler	143.2	141 - 182	146 -	−1.15	−10.04
		164.1		182	−5.45	
		178.1			−3.44	
TPE_4	30 PS + 50 NR + 20 OPEFB carbon filler	138.9	137 - 186	141 -	−5.23	−27.86
		152.6		186	−7.88	
		164.5			−13.42	
		184.3			−1.33	
TPE_5	30 PS + 45 NR + 25 OPEFB carbon filler	147.0	146 - 169	149 -	−10.46	−23.86
		153.9		173	−0.75	
		170.3			−12.65	

4. Conclusion

In conclusion, the analysis results showed that the best composites based on thermal stability were TPE_1 and TPE_2, with PS-g-MA/NR/OPEFB carbon filler compositions of (30:65:5) wt% and (30:60:10) wt%, respectively. This is shown by the composite thermal stability ($T_{5\%}$) values of 360°C and 363°C, respectively. However, based on the morphological test, the best composite, TPE_4, exhibited smaller surface voids, reduced PS and NR agglomerates, as well as increased adhesion, as shown by a total ΔH of −27.86 J/g. Meanwhile, TPE_5 exhibited a homogeneous filler dispersion and no voids formed, but experienced a decrease in thermal stability, as shown by a total ΔH of −23.86 J/g. This suggests that a 20% carbon filler provides the optimal balance between interfacial interactions and phase dispersion. Each composite formulation exhibits distinct strengths and limitations, although further investigation is required to identify the most suitable composition for specific applications. It is recommended that additional mechanical testing, such as tensile strength, elongation at break, and resistance to moisture, oxidation, solvents, and UV exposure, be conducted to evaluate the long-term stability of the composites.

AI Usage Statements

During the preparation of this manuscript, the authors used ChatGPT (GPT-5.5, developed by OpenAI) for assist in language refinement, grammar checking, sentence restructuring, paraphrasing, and improving the clarity and readability of the manuscript. All AI-generated outputs were critically reviewed and thoroughly edited by the authors to ensure factual accuracy, clarity of expression, and compliance with academic standards. The authors take full responsibility for the integrity and content of this manuscript.

CRediT Authorship Statement

Indah Agus Setiorini : Conceptualization, Methodology, Formal Analysis, Data Curation, Writing – Original Draft, Writing – Review & Editing, Visualization, Project Administration. **Achmad Faisal Faputri**: Investigation, Formal Analysis, Validation, Data Curation TPE. **Rahma Nuryanti**: Validation, Data Curation and Investigation filler. **Amiliza Miarti** : Supervision, Validation. **Muhammad Rasyad Hilmi :** Resources, Supervision, Validation. **Hasrinah Hasbullah:** Supervision, Validation

Declaration of competing interest

The authors declare there are no conflict of interest

Acknowledgments

The authors express their sincere gratitude to the Ministry of Higher Education, Science, and Technology of the Republic of Indonesia for the financial support provided under the 2025 Beginner Lecturer Research Grant scheme. This funding contributed significantly to the successful completion of this research.

References

[1] Tajeddin, B., & Arabkhedri, M. (2020). *Polymers and food packaging. Polymer Science and Innovative Applications: Materials, Techniques, and Future Developments*. INC. doi: 10.1016/B978-0-12-816808-0.00016-0

[2] Dehnou, K.H., & Hadianfard, M. J. (2024). Enhancing Thermal, Viscoelastic, and Mechanical Properties

of Silicone Rubber Matrix through Reinforcements for Use as a Medical Implant. *Recent Progress in Materials*, 06(02), 1–30. doi: 10.21926/rpm.2402011

[3] Petrény, R., Tóth, C., Horváth, A., & Mészáros, L. (2022). Development of electrically conductive hybrid composites with a poly(lactic acid) matrix, with enhanced toughness for injection molding, and material extrusion-based additive manufacturing. *Heliyon*, 8(8). doi: 10.1016/j.heliyon.2022.e10287

[4] Rejab, N.A., Akindoyo, J.O., & Jaafar, M. (2022). Flexural properties of recycled polystyrene composite laminates reinforced with MWCNT filled kenaf fiber. *Materials Today: Proceedings*, 66, 2900–2903. doi: https://doi.org/10.1016/j.matpr.2022.06.554

[5] Li, H., Wang, G., Wu, Y., Jiang, N., & Niu, K. (2024). Functionalization of Carbon Nanotubes in Polystyrene and Properties of Their Composites: A Review. *Polymers*, 16(6). doi: 10.3390/polym16060770

[6] Tutek, K., Kosmalska-olańska, A., Masek, A., Tutek, K., Kosmalska-olańska, A., & Masek, A. (2025). Thermoplastic Elastomer (TPE) Composites with Modified Fibers and Hemp Shives – an Ecological Approach to Modern Polymer Materials Thermoplastic Elastomer (TPE) Composites with Modified Fibers and Hemp Shives – an Ecological Approach to Modern Polymer M. *Journal of Natural Fibers*, 22(1). doi: 10.1080/15440478.2025.2473466

[7] Nuriskasari, I., Syahrial, A. Z., Ivandini, T. A., Sumboja, A., Priyono, B., Yan, Q., … Priyono, S. (2024). Synthesis of graphitic carbon from empty palm oil fruit bunches through single-step graphitization process using K2FeO4-KOH catalyst as lithium ion battery anode. *Results in Engineering*, 24(October), 103273. doi: 10.1016/j.rineng.2024.103273

[8] Sakamoto, T., Ahmad Zaini, M. A., Amano, Y., & Machida, M. (2021). Preparation and characterization of activated carbons produced from oil palm empty fruit bunches. *Carbon*, 175, 611. doi: https://doi.org/10.1016/j.carbon.2021.01.072

[9] Tayouri, M. I., Estaji, S., Mousavi, S. R., Yazdanbakhsh, A., Nouranian, S., Ruckdäschel, H., & Khonakdar, H. A. (2023). Polystyrene/Polyolefin Elastomer Blends Loaded with Halloysite Nanotubes: Morphological, Mechanical, and Gas Barrier Properties. *Macromolecular Materials and Engineering*, 308(9), 1–17. doi: 10.1002/mame.202300080

[10] Karunanayake, L., Etampawala, T., de Silva, D. J., Bandara, J., Rajapaksha, A. U., & Vithanage, M. (2025). Role and potential of biochar as a sustainable alternative reinforcing filler to carbon black in rubber composites. *Biochar*, 7(1). doi: 10.1007/s42773-025-00429-3

[11] Goodarzi, M., Pircheraghi, G., Khonakdar, H. A., & Altstadt, V. (2022). Flexible high dielectric polystyrene/ethylene-α-octene copolymer/graphene nanocomposites: Tuning the morphology and dielectric properties by graphene's surface polarity. *Polymers for Advanced Technologies*, 33(3), 937–951. doi: https://doi.org/10.1002/pat.5569

[12] Entezam, M., Poormadadkar, H., Khonakdar, H. A., & Jafari, S. H. (2020). Melt rheology and interfacial properties of binary and ternary blends of PS, EOC, and SEBS. *Journal of Applied Polymer Science*, 137(23), 48791. doi: https://doi.org/10.1002/app.48791

[13] Kiani, F., Entezam, M., Khonakdar, H. A., Jafari, S. H., Callsen, C., & Altstädt, V. (2020). Assessment of compatibilization role of nanoclay in immiscible polystyrene/ethylene–octene copolymer blends via wide-angle X-ray scattering, microstructure, rheological analyses, and mechanical properties. *Journal of Applied Polymer Science*, 137(22), 48748. doi: https://doi.org/10.1002/app.48748

[14] Sharma, T., & Garg, M. (2023). Effect of ZnO nanoparticles and temperature on dielectric constant/loss properties of polystyrene nanocomposite films. *The European Physical Journal Plus*, 138(7), 611. doi: 10.1140/epjp/s13360-023-04250-4

[15] Zhang, Z., Cao, H., Quan, Y., Ma, R., Pentzer, E. B., Green, M. J., & Wang, Q. (2022). Thermal Stability and Flammability Studies of MXene–Organic Hybrid Polystyrene Nanocomposites. *Polymers*, 14(6), 1–10. doi: 10.3390/polym14061213

[16] Liu, X., Qin, Y., Zhao, S., & Dong, J.-Y. (2021). Nanocomposites-Turned-Nanoalloys Polypropylene/Multiwalled Carbon Nanotubes-graft-Polystyrene: Synthesis and Polymer Nanoreinforcement. *Industrial & Engineering Chemistry Research*, 60(28), 10167–10179. doi: 10.1021/acs.iecr.1c01362

[17] Hidayani, T. R., Wirjosentono, B., Nasution, D. Y., & Tamrin. (2023). Preparation and Characterization of Sound-Absorbent Based on Polystyrene Reinforced Primary Sludge and Fly Ash from Pulp Mill.

International Journal of Technology, 14(3), 649–658. doi: 10.14716/ijtech.v14i3.5131

[18] Atmakuri, A., Palevicius, A., Vilkauskas, A., & Janusas, G. (2022). Numerical and Experimental Analysis of Mechanical Properties of Natural-Fiber-Reinforced Hybrid Polymer Composites and the Effect on Matrix Material. *Polymers*, 14(13). doi: 10.3390/polym14132612

[19] Mechanics, A., Nanda, S., Andrianto, K., Maulana, J., Eden, O., Riyanto, S., … Fahrozy, M. (2026). Jurnal Mekanik Terapan Analisis Sifat Mekanik dan Penyerapan Air Komposit Polyester Berbasis Serat Alami, 06(03), 172–180. doi: 10.32722/jmt.v6i3.7978

[20] Peña-Alcántara, A., Nikzad, S., Michalek, L., Prine, N., Wang, Y., Gong, H., … Bao, Z. (2023). Effect of Molecular Weight on the Morphology of a Polymer Semiconductor–Thermoplastic Elastomer Blend. *Advanced Electronic Materials*, 9(9). doi: 10.1002/aelm.202201055

[21] Tian, A., Zhang, J., & Wang, Y. (2025). Miscibility, Thermal, and Mechanical Properties of Recycled Waste Tire Rubber-Modified Polystyrene Sustainable Composites. *BioResources* . doi: 10.15376/biores.20.1.1273-1285

[22] Hashim, F., Surya, I., Rusli, A., & Ismail, H. (2022). Microstructure-properties of dynamically vulcanized mengkuang leaf fibre/ethylene vinyl acetate/natural rubber thermoplastic elastomer composites. *BioResources*, 17(4), 6036–6055. doi: 10.15376/biores.17.4.6036-6055

[23] Ma, Y., Yang, K., Zhang, Y., Wang, J., Zeng, S., & Huang, X. (2024). Mechanical properties and thermal stability of high-temperature (cooking temperature)-resistant PP/HDPE/POE composites. *E-Polymers*, 24(1). doi: 10.1515/epoly-2023-0164

[24] Seier, M., Stanic, S., Koch, T., & Archodoulaki, V. M. (2020). Effect of different compatibilization systems on the rheological, mechanical and morphological properties of polypropylene/polystyrene blends. *Polymers*, 12(10), 1–20. doi: 10.3390/polym12102335

[25] Fitriana, I., Ratnasari, D., Ismoyojati, R., & Febriansyah, I. (2024). Journal of Sustainable Agriculture and Biosystems Engineering Chemical Characteristics of Palm Frond and Empty Fruit Bunch Biochar in Pyrolysis Method, 02(01), 28–33.

[26] Marhani, Sahur, A., Laban, S., & Musa, Y. (2022). Characterization of Biochar Empty Fruit Bunches OPEFB at Various Temperatures and Burning Time. *Journal of Experimental Biology and Agricultural Sciences*, 10(3), 599–606. doi: 10.18006/2022.10(3).599.606

[27] Bolanakis, N., Maravelakis, E., Papadakis, V., Kalderis, D., Michailidis, N., Argyros, A., … Vidakis, N. (2025). Valorization of Biochar as a Reinforcement Agent in Polyethylene Terephthalate Glycol for Additive Manufacturing: A Comprehensive Content Optimization Course. *Journal of Manufacturing and Materials Processing*, 9(2). doi: 10.3390/jmmp9020068

[28] Paula, R., Carvalho, J., Júnior, A., Fagundes, F., de Lima, R., Lima, E., … Machado, A. (2025). Analysis of Biochar–Cement Composites by SEM/EDS: Interfacial Interactions and Effects on Mechanical Strength. *C-Journal of Carbon Research*, 11(3), 1–14. doi: 10.3390/c11030045

[29] Mahardika, M., Zakiyah, A., Ulfa, S. M., Ilyas, R. A., Hassan, M. Z., Amelia, D., … Norrrahim, M. N. F. (n.d.). No TitleRecent Developments in Oil Palm Empty Fruit Bunch (OPEFB) Fiber Composite. *Journal of Natural Fibers*. doi: https://doi.org/10.1080/15440478.2024.2309915

[30] Md Noh, N. H., & Wusko, I. (2020). Characterization and Analysis of Oil Palm Empty Fruit Bunch (OPEFB) Waste of PT Kharisma Alam Persada South Borneo. *Majalah Obat Tradisional*, 25. doi: 10.22146/mot.52715

[31] Haile, L. (2021). Study of Recycling of Waste High Impact Polystyrene (PS-HI) and Polystyrene with Flame Retardant Additives (PS-FR) Co-Polymers. *Journal of Textile Science & Fashion Technology*, 7(4), 1–11. doi: 10.33552/jtsft.2021.07.000666

[32] Phoncharoen, V., & Pianthong, K. (2025). Investigation on Yield of Natural Rubber to Bio-Crude Oil from Hydrothermal Liquefaction Process. *Journal of Research and Applications in Mechanical Engineering*, 13(1), 1–10. doi: 10.14456/jrame.2025.5

[33] Setiorini, I. A. (2020). Karakteristik Termoplastik Elastomer Dari Karet Alam Dan Polipropilena Dengan Penambahan Carbon Black Filler. *Jurnal Teknik Patra Akademika*, 10(02), 41–44. doi: 10.52506/jtpa.v10i02.93

[34] Saleh, T. A. (2022). Chapter 8 - Properties of nanoadsorbents and adsorption mechanisms. In T. A. Saleh (Ed.), *Surface Science of Adsorbents and Nanoadsorbents* (Vol. 34, pp. 233–263). Elsevier. doi:

https://doi.org/10.1016/B978-0-12-849876-7.00010-5

[35] Oktaviani, Z., Wahyuni, D., & Nurhanisa, M. (2024). Sintesis Karbon Aktif dari Tandan Kosong Kelapa Sawit dengan Aktivator Gelombang Mikro dan Pengujian Kualitas Berdasarkan SNI 06-3730-1995. *Newton-Maxwell Journal of Physics*, 5(1). doi: 10.33369/nmj.v5i1.33499

[36] Tanasă, F., Zănoagă, M., Teacă, C.-A., Nechifor, M., & Shahzad, A. (2020). Modified hemp fibers intended for fiber-reinforced polymer composites used in structural applications—A review. I. Methods of modification. *Polymer Composites*, 41(1), 5–31. doi: https://doi.org/10.1002/pc.25354

[37] Das, C., Tamrakar, S., Kiziltas, A., & Xie, X. (2021). Incorporation of biochar to improve mechanical, thermal and electrical properties of polymer composites. *Polymers*, 13(16), 1–32. doi: 10.3390/polym13162663

[38] Fan, Y., Fowler, G. D., & Zhao, M. (2020). The past, present and future of carbon black as a rubber reinforcing filler – A review. *Journal of Cleaner Production*, 247, 119115. doi: https://doi.org/10.1016/j.jclepro.2019.119115

[39] Okoye, C. O., Jones, I., Zhu, M., Zhang, Z., & Zhang, D. (2021). Manufacturing of carbon black from spent tyre pyrolysis oil – A literature review. *Journal of Cleaner Production*, 279, 123336. doi: https://doi.org/10.1016/j.jclepro.2020.123336

[40] Chang, B. P., Gupta, A., Muthuraj, R., & Mekonnen, T. H. (2021). Bioresourced fillers for rubber composite sustainability: current development and future opportunities. *Green Chem.*, 23(15), 5337–5378. doi: 10.1039/D1GC01115D

[41] Kalogeras, I. M. (2016). *Glass-Transition Phenomena in Polymer Blends*. *Encyclopedia of Polymer Blends: Volume 3: Structure* (Vol. 3). doi: 10.1002/9783527653966.ch1

[42] Ucpinar, B., Sivrikaya, T., & Aytac, A. (2025). Sustainable hemp fiber reinforced polylactic acid/poly(butylene succinate) biocomposites: Assessing the effectiveness of MAH-g-PLA as a compatibilizer. *Polymer Composites*, 46(10), 9438–9453. doi: 10.1002/pc.29569

[43] Guo, Y., Ruan, K., Shi, X., Yang, X., & Gu, J. (2020). Factors affecting thermal conductivities of the polymers and polymer composites: A review. *Composites Science and Technology*, 193, 108134. doi: https://doi.org/10.1016/j.compscitech.2020.108134

[44] Ruan, K., Shi, X., Guo, Y., & Gu, J. (2020). Interfacial thermal resistance in thermally conductive polymer composites: A review. *Composites Communications*, 22, 100518. doi: https://doi.org/10.1016/j.coco.2020.100518